Environmental Science & Technology

Article

pubs.acs.org/est

What's in an EEM? Molecular Signatures Associated with Dissolved Organic Fluorescence in Boreal Canada

A. Stubbins,*[,†] J.-F. Lapierre,[‡] M. Berggren,[‡,§] Y. T. Prairie,[‡] T. Dittmar,[⊥] and P. A. del Giorgio[‡]

[†]Skidaway Institute of Oceanography, Marine Sciences Department, University of Georgia, Savannah, Georgia 31401, United States

[‡]Département des Sciences Biologiques, Université du Québec à Montréal, Case Postale 8888, succursale Centre-Ville, Montréal, Quebec H3C 3P8, Canada

[§]Department of Physical Geography and Ecosystem Science, Lund University, SE-223 62 Lund, Sweden

[⊥]Research Group for Marine Geochemistry, Institute for Chemistry and Biology of the Marine Environment (ICBM), University of Oldenburg, Carl-von-Ossietzky-Strasse 9-11, D-26129 Oldenburg, Germany

Supporting Information

ABSTRACT: Dissolved organic matter (DOM) is a master variable in aquatic systems. Modern fluorescence techniques couple measurements of excitation emission matrix (EEM) spectra and parallel factor analysis (PARAFAC) to determine fluorescent DOM (FDOM) components and DOM quality. However, the molecular signatures associated with PARAFAC components are poorly defined. In the current study we characterized river water samples from boreal Québec, Canada, using EEM/PARAFAC analysis and ultrahigh resolution mass spectrometry (FTICR-MS). Spearman's correlation of FTICR-MS peak and PARAFAC component relative intensities determined the molecular families associated with 6 PARAFAC components. Molecular families associated with PARAFAC components numbered from 39 to 572 FTICR-MS derived elemental formulas. Detailed molecular properties for each of the classical humic- and protein-like FDOM components are presented. FTICR-MS formulas assigned to PARAFAC components represented 39% of the total number of formulas identified and 59% of total FTICR-MS peak intensities, and included significant numbers compounds that are highly unlikely to fluoresce. Thus, fluorescence measurements offer insight into the biogeochemical cycling of a large proportion of the DOM pool, including a broad suite of unseen molecules that apparently follow the same gradients as FDOM in the environment.

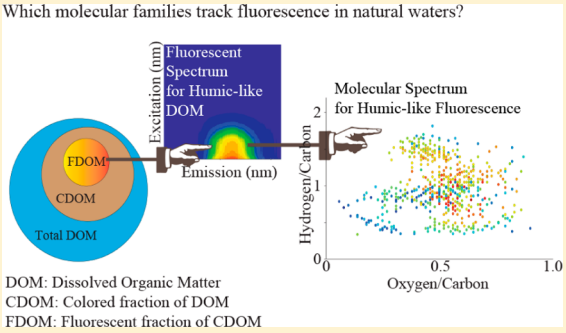

1. INTRODUCTION

Dissolved organic matter (DOM) is a key constituent within aquatic ecosystems,[1] attenuating light,[2] initiating photoreactions,[3] influencing metal and pollutant transport and bioavailability,[4,5] and connecting soil organic carbon stores to those of the ocean.[6] The aromatic fraction of the DOM pool is colored (CDOM),[7,8] and a subfraction of CDOM fluoresces (fluorescent DOM; FDOM).[9] FDOM excitation emission matrix spectra (EEMS) reveal fluorescence features that provide information about DOM source, diagenetic state, reactivity, ecological function and chemistry.[9−13] Early studies defined these features using peak picking techniques,[9,10] whereas current research predominantly utilizes a statistical fitting approach—parallel factor analysis (PARAFAC)—to define fluorescent components.[14] As the components determined by PARAFAC are unique to the sample set analyzed, it is useful to compare PARAFAC components to the classically defined fluorescence peaks commonly found in natural DOM.

Due to the simplicity and low cost of fluorescence measurements, they are increasingly applied to assess DOM quality, with 276 articles published in 2013 (Web of Science search terms fluorescen* and "dissolved organic matter"). However, the chemistry and percentage of DOM molecules that fluoresce remain ill-defined. Furthermore, the quantity and quality of nonfluorescing DOM molecules that track fluorescence components in natural waters is also unknown. This latter gap in knowledge is of significance to scientists using FDOM as a prism through which to interpret the broader DOM pool, and is the primary topic addressed in the current study.

In the progression toward a molecular understanding of DOM, ultrahigh resolution Fourier transform ion cyclotron mass spectrometry (FTICR-MS) is offering novel insight and fostering greater recognition of DOM's complexity.[15,16] FTICR-MS resolves thousands of peaks within a single DOM sample so precisely that elemental formulas (i.e., $C_nH_nO_nN_nS_n$) can be assigned. Although resolved by elemental formula,

Received: April 29, 2014
Revised: August 13, 2014
Accepted: August 22, 2014
Published: August 22, 2014

Table 1. Excitation and Emission Maxima, Descriptors and Relation to the Nomenclature of Coble et al.[9,33] for PARAFAC Components P1 to P6 and their Biogeographic Distribution and Lability as Defined by Lapierre et al.[19]

PARAFAC component	Exc:Em maxima (nm:nm)	corresponding classical peak	nomenclature; assumed properties	assumed biolability	assumed photolability
P1	<275(295):420	Peak A	humic-like highly processed terrigenous	low	high
P2	<275:480	shoulder of Peak A	humic-like highly processed terrigenous	low	high
P3	<345(275):430	Peak C(Peak A)	humic-like less processed terrigenous	moderate	highest
P4	335:440	Peak C/M	marine/aquatic humic-like terrigenous; autochthonous; microbially processed	high	moderate; also photoproduced
P5	300:390	Peak M/N	aquatic humic-like terrigenous; autochthonous; microbially processed	high	moderate
P6	275:336	Peak B+T	amino acid-like freshly added to the environment from autochthony, land or microbes	highest	moderate

FTICR-MS does not directly resolve DOM structure. Thus, each FTICR-MS peak likely contains many different structural isomers, each with different sources, sinks, and ecological roles.

In this study, we determined FTICR mass spectra and the PARAFAC fluorescence components for 22 DOM samples from boreal rivers spanning a wide range in chemical, watershed, and DOM properties. The molecular families associated with each PARAFAC component are described.

2. MATERIALS AND METHODS

2.1. Sample Collection and Processing. We sampled 11 boreal rivers and streams in the Abitibi region, Quebec, Eastern Canada, covering a large range in Strahler stream order (1−6), DOM concentration, and CDOM absorption (Supporting Information (SI) Table S1). Rivers were sampled under contrasting hydrology, yielding a total of 22 samples and increasing the diversity of samples (SI Table S1). Water was filtered on-site (0.45 μm; Sarstedt), stored cold and dark in acid-washed glass vials (<1 month) until DOC and optical analyses. Samples for FTICR-MS were frozen until analysis.

2.2. Dissolved Organic Carbon and Optical Characterization. Dissolved organic carbon (DOC) was measured in duplicate on an OI Analytical TIC/TOC Analyzer. Standards were prepared using sodium phthalate. The coefficient of variation of duplicates, average precision, and average accuracy relative to standards were 2%, 0.1 mg-C L^{-1} at 5 mg-C L^{-1}, and 3% or 0.15 mg-C L^{-1} at 5 mg-C L^{-1}, respectively.

CDOM absorbance spectra (190−900 nm) were recorded using a 2 cm quartz cell and an Ultrospec 2100 ultraviolet−visible spectrometer (Biochrom). Ultrapure water (Milli-Q) blank-corrected spectra were further corrected by subtraction of the average absorbance between 700 and 800 nm.[17] Data were converted to Napierian absorption coefficients, a (m^{-1}).[18] Specific Ultraviolet Absorbance (SUVA; mg-C L^{-1} m^{-1}) was calculated as the Decadic absorption coefficient at 254 nm (m^{-1}) divided by DOC concentration (mg-C L^{-1}).[7]

EEM spectra were measured in 1 cm quartz cells in a RF5301 PC spectrofluorometer (Shimadzu; SI S1a). The 22 samples analyzed by FTICR-MS in the current study were selected from a set of over 1000 samples from lakes, rivers, ponds, and wetlands in boreal Québec, Canada (see ref 19). A PARAFAC model was developed for this full data set[19] using Matlab DOMfluor 1.7.[14] Consequently, the PARAFAC components presented here represent fluorescent properties that are widespread across boreal aquatic ecosystems.[19] For further details see SI S1a.

2.3. Solid Phase Extraction and Mass Spectrometry. Further details of the extraction and FTICR-MS methods are in SI S1b. In brief: Electrospray ionization (ESI) of DOM is sensitive to sample matrix. Thus, samples were solid phase extracted (SPE) using Varian Bond Elut PPL to generate pure DOM isolates.[20] At the University of Oldenburg, methanol PPL-DOM extracts were mixed 1:1 (v:v) with ultrapure water and infused into the ESI source of a 15 T FTICR-MS (Solarix Bruker). Molecular formulas were assigned to peaks with signal-to-noise ratios >5 based on published rules.[21−23] Peaks below a standardized detection limit were filled to prevent false negatives for the absence of a peak within samples with low dynamic range.

Assigned formulas were categorized by compound class based upon elemental stoichiometries.[24] Modified aromaticity index (AI_{mod})[25] values were calculated as follows:

$$AI_{mod} = (1 + C - 0.5O - S - 0.5H) / (C - 0.5O - S - N - P)$$

AI_{mod} values 0.5 to 0.67 and >0.67 were assigned as aromatic and condensed aromatic structures, respectively.[25] Further compound classes were defined as follows: highly unsaturated, low oxygen = AI_{mod} < 0.5, H/C < 1.5, O/C < 0.5; highly unsaturated, high oxygen = AI_{mod} < 0.5, H/C < 1.5, O/C 0.5−0.9; aliphatics = H/C 1.5−2.0, O/C < 0.9, N = 0; peptides = H/C 1.5−2.0, O/C < 0.9 and N > 0; sugars = O/C > 0.9. Although consistent with peptide and sugar stoichiometries, the last two assignments are ambiguous as the formulas may also occur in alternative isomeric arrangements.

2.4. Spearman's Correlation Coefficient. PARAFAC component intensities were normalized to the sum of component fluorescence intensities for a given sample. The intensities of FTICR-MS peaks were normalized to the total intensity of all peaks to which formulas were assigned within a sample. Relative intensities of FTICR-MS peaks across samples were not normally distributed, precluding use of Pearson's correlations. Therefore, Spearman's correlations were derived between FTICR-MS and PARAFAC data (JMP Pro 11.0.0 SAS). For an n of 22 samples, a Spearman's coefficient (r) of 0.49 was calculated to be significant at the 99% confidence limit (Student's t test; see SI S1c). Thus, molecular formulas correlated to PARAFAC component intensities across the 22 samples with Spearman's $r \geq 0.49$ were assigned to each PARAFAC component. A similar approach was applied in ref 21.

3. RESULTS AND DISCUSSION

3.1. Concentrations and Optical Properties. Concentrations of DOC varied by a factor of 4, from 4.6 to 19.8 mg-C L^{-1}, a_{254}CDOM by a factor of ∼28, from 9 to 250 m^{-1}, and SUVA by a factor of 17, from 0.4 to 6.3 mg-C L^{-1} m^{-1} (SI

Table 2. Number of Formulas, Average Molecular Weights (MWs), and Structural Groupings of Molecular Formulas As Determined by Fourier Transform Ion Cyclotron Mass Spectrometry Found within the Suite of 22 River Water Samples (All); Found to Correlate with Each of the Six Fluorescence PARAFAC Components Identified (P1 to P6); and Those Which Did Not Correlate with Any of the PARAFAC Components (No Correlation)[a]

	all	no correlation	P1	P2	P3	P4	P5	P6
no. total formulas	4109	2517	556	39	223	333	572	244
(% of intensity)	(100%)	(41%)	(12%)	(1%)	(18%)	(9%)	(28%)	(12%)
average MW (Da.)	450	468	536	414	445	316	369	282
(intensity weighted)	(379)	(391)	(397)	(372)	(424)	(329)	(378)	(279)
no. formulas without N	2547	1539	506	39	181	72	175	169
(% of intensity)	(100%)	(41%)	(13%)	(1%)	(20%)	(7%)	(26%)	(13%)
no. formulas with N	1562	978	50	0	42	261	397	75
(%)	(100%)	(44%)	(1%)	(0%)	(1%)	(33%)	(42%)	(9%)
black carbon	165	53	95	3	1	8	6	4
(% of black carbon)	(100%)	(21%)	(65%)	(2%)	(0%)	(7%)	(4%)	(5%)
aromatic	845	547	151	8	8	84	76	37
(% of aromatic)	(100%)	(42%)	(40%)	(0%)	(0%)	(8%)	(6%)	(15%)
highly unsaturated	2752	1682	285	23	213	224	480	138
(% of highly	(100%)	(41%)	(8%)	(1%)	(22%)	(9%)	(32%)	(11%)
aliphatics	282	177	25	0	1	15	10	65
(% of aliphatics)	(100%)	(63%)	(9%)	(0%)	(0%)	(5%)	(4%)	(23%)
sugars	51	46	0	5	0	0	0	0
(% of sugars)	(100%)	(89%)	(0%)	(8%)	(0%)	(0%)	(0%)	(0%)
peptides	14	12	0	0	0	2	0	0
(% of peptides)	(100%)	(99%)	(0%)	(0%)	(0%)	(1%)	(0%)	(0%)

[a]For MW, values in parentheses report intensity weighted average MW. All other values in parentheses represent the percentage of peak intensity contributed by each classification of molecular formulas. Note that the summation of percentages from P1 to P6 in each row does not correspond to 100% because components share some molecular formulas.

Table S1). This encompasses a wide range of the spectrum observed for rivers, lakes, and wetlands for boreal Québec and Eastern Canada.[26,27] Looking further afield, average a_{254}CDOM levels across 30 major U.S. rivers ranged from 6 to 442 m^{-1} and SUVA from 1.3 to 4.6 mg-C L^{-1} m^{-1}, with DOC concentrations in rivers globally typically between 0.5 and 50 mg-C L^{-1}.[28,29] Thus, SUVA, DOC and *a*CDOM values in the 22 samples studied covered a wide range of the values found in rivers globally. The wide range in SUVA values for the 22 selected samples indicates the samples' DOM varied significantly in its optical properties.[7]

The PARAFAC model included 1349 samples from across boreal Québec and resolved six fluorescent components (SI Figures S1−S3; Table 1).[19] The components are listed from P1 to P6 in order of their contribution toward the sample set's total fluorescence intensity. The PARAFAC model, together with the biolability and photolability of the identified fluorescence components are described in ref 19.

Peaks A and C, the two predominant terrigenous humic-like fluorescence peaks in the literature,[9,13] are represented by P1 and P3, respectively (SI Figures S1−S3; Table 1). Peaks A and C are near-ubiquitous in aquatic environments, reaching highest levels in rivers draining wetland and forested catchments, and are associated with highly aromatic, high molecular weight (MW) DOM.[12] An additional, apparently terrigenous humic-like fluorescence component was identified (P2), with an emission peak shifted to slightly longer wavelengths than Peak A and C (SI Figure S1−S3). Of these three humic-like components, P3 was the most photolabile,[19] possibly because its excitation maximum extends furthest into the solar spectrum[30] (Table 1; SI Figure S1).

P4 fell close to Peak C, with a shoulder extending toward Peak M and a secondary maximum near Peak A. P5's maximum intensity lay between Peaks M and N (SI Figure S1−S3; Table 1). Peaks M and N are commonly reported to be of mixed−terrigenous, autochthonous, and microbially reworked−source.[12] Peak M is further described as low MW.[12] Peak N can be rapidly biodegraded by bacteria.[31,32] PARAFAC components P4 and P5 may also represent fresh inputs of DOM from terrigenous sources, due to their prevalence in brown waters throughout boreal Québec.[19] P6 was the main driver of DOC biolability across lakes, rivers and wetlands in boreal Québec[19] and represents Peak B and T (SI Figure S1−S3; Table 1), which are classically interpreted as representing protein-like, nitrogen-rich, low MW, highly biolabile DOM.[9,33] However, other studies have shown that N-free low molecular weight aromatics (e.g., gallinic acid) also fluoresce in this region.[34]

3.2. Molecular Signatures of Boreal River DOM. FTICR-MS enabled the assignment of molecular formulas to 4109 peaks (Table 2 and SI Table S2), demonstrating the molecular complexity of boreal river DOM. Nitrogen-free peaks accounted for 61% of formulas and 91% of the intensity of all formulas (Table 2). Nitrogen-containing formulas (Table 2) accounted for 38% of peaks and 9% of total intensity. The 485 molecular formulas containing S represented 12% of peaks or 3% of intensity.

Elemental formulas were used to estimate molecular structural classes (Section 2.3). Dissolved black carbon (condensed aromatics) accounted for 165 formulas (1% of intensity), aromatics for 845 formulas (11% of intensity), and aliphatics for 282 formulas (4% of intensity; Table 2). Highly unsaturated formulas were the most prevalent (2752 formulas, 84% of intensity). Elemental formulas classified as highly unsaturated cover a range of possible structural isomers with varying biogeochemical qualities. For instance, lignin-colored,

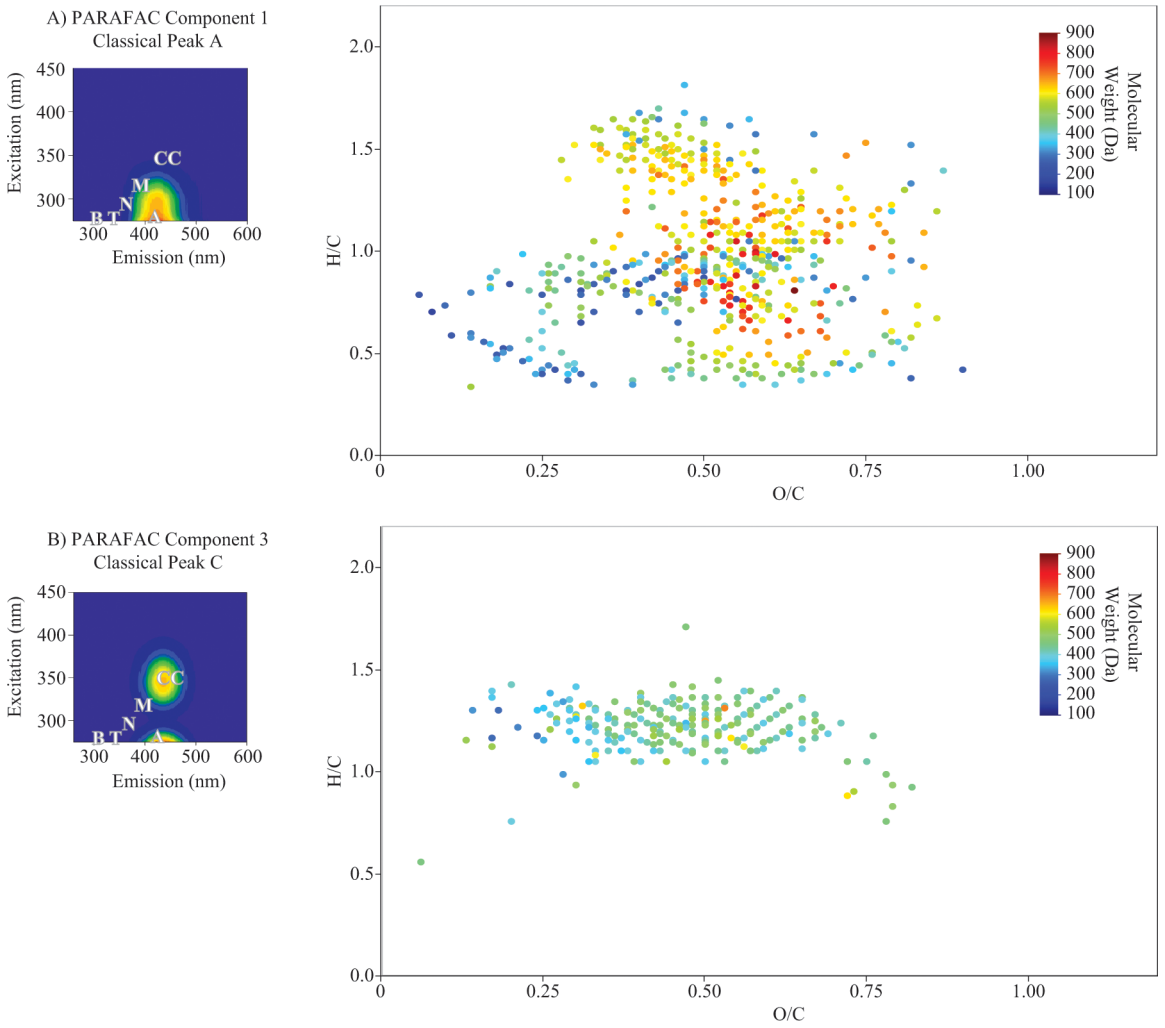

Figure 1. Excitation emission spectra (EEMS) and van Krevelen plots for PARAFAC components P1 and P3. In the EEMS, color indicates fluorescence intensity and bold white text the approximate positions of the classical fluorescent dissolved organic matter Peak A, C, M, N, B, and T defined in the text. The van Krevelen plots show the molecular families associated with each PARAFAC component and data points are colored by molecular weight. Panels A and B represent PARAFAC components 1 and 3, respectively.

Table 3. Numbers of Formulas and Percentages of Mass Spectral Peak Intensity Shared between Each PARAFAC Component

	P1	P2	P3	P4	P5	P6
no. of formulas shared with P1	556	1	0	0	0	12
(% of intensity)	(100%)	(<1%)	(0%)	(0%)	(0%)	(5%)
no. of formulas shared with P2	1	39	15	0	0	0
(% of intensity)	(<1%)	(100%)	(7%)	(0%)	(0%)	(0%)
no. of formulas shared with P3	0	15	223	0	77	0
(% of intensity)	(0%)	(39%)	(100%)	(0%)	(14%)	(0%)
no. of formulas shared with P4	0	0	0	333	224	45
(% of intensity)	(0%)	(0%)	(0%)	(100%)	(39%)	(18%)
no. of formulas shared with P5	0	0	77	224	572	7
(% of intensity)	(0%)	(0%)	(35%)	(67%)	(100%)	(3%)
no. of formulas shared with P6	12	0	0	45	7	244
(% of intensity)	(2%)	(0%)	(0%)	(14%)	(1%)	(100%)

photolabile and biolabile, aromatic biomarkers of terrestrial land plants[23,35−37]—and carboxylic-rich alicyclic molecules (CRAM)—noncolored, biorefractory carboxylic-rich alicyclic molecules of potential microbial origin[16]—both have elemental stoichiometries that fall in this class despite differences in their structure, source and biogeochemical reactivity. Given the terrigenous nature of DOM in the current samples, most of the highly unsaturated formulas identified are likely plant and soil derived, with some aromatic/lignin-like character. However, a portion of these peaks' intensities may have been contributed by aromatic-free isomers, such as CRAM. Few formulas were assigned as sugars (51 formulas, <1% of intensity) and peptides (14 formulas, <1% of intensity). These patterns, as well as the

dx.doi.org/10.1021/es502086e | Environ. Sci. Technol. 2014, 48, 10598−10606

MWs (Table 2), are broadly consistent with previous FTICR-MS studies of riverine DOM.[23,37,38]

3.3. Relating PARAFAC Components to Molecular Formulas. The elemental formulas associated with each PARAFAC component are listed in SI Table S2. Utilizing Spearman's rank correlations at the 99% confidence limit (Section 2.4), 39% of molecular formulas and 59% of peak intensities were assigned to one or more PARAFAC components (Table 2). Thus, PARAFAC components apparently deliver information about the gradients for more than half the DOM within the analytical window of coupled PPL extraction and negative ionization ESI FTICR-MS. The molecular formulas that did not correlate with any PARAFAC component were enriched in aliphatic and sugar formulas that are not expected to absorb light or fluoresce, and were depleted in condensed aromatic moieties that are known components of CDOM.[39] Individual PARAFAC components were ascribed between 39 and 572 formulas (Table 2). The information-richness contained in each molecular family assigned to a PARAFAC component is apparent by the widespread of data in van Krevelen plots (Figure 1 and SI Figure S3).

The use of Spearman's correlations purposefully allowed molecular formulas to correlate with one or more PARAFAC components as a given FTICR-MS molecular formula can include many different structural isomers. P4 and P5 shared the most formulas. Of the 333 formulas assigned to P4, 224 (67% of P4 formulas) were shared with P5 (Table 3). These 224 shared formulas represented 39% of the 572 formulas assigned to P5. P1 was assigned 556 formulas, and shared the least number (13) and percentage (2%) of formulas with other PARAFAC components (Table 3).

A MANOVA on 3 molecular characteristics (MW, modified aromaticity index, and nitrogen content) revealed that the molecular formulas associated with each PARAFAC component represented statistically different families (contrast analysis of the MANOVA fit data, $p < 0.0001$). A canonical centroid plot shows that these molecular families separate mostly on the basis of N content and MW, and confirmed that the P4 and P5 molecular families are more similar to one another than any other two molecular families (Figure 2). The P2 and P3 molecular families also plot close to one another, supporting the conclusion reached from the optical signatures (Section 3.1) that P2 represents terrestrial humic-like DOM.

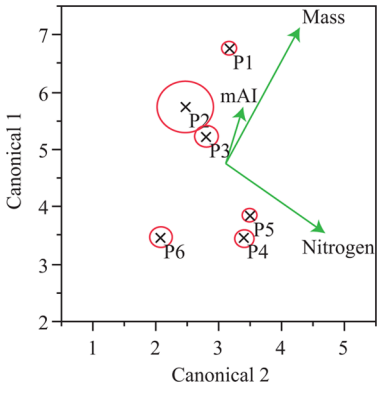

Figure 2. Centroid canonical plot from the MANOVA run on 3 characteristics derived from the elemental formulas (molecular weight, modified aromaticity index, and nitrogen content) of the molecular families associated with each PARAFAC component. Multivariate contrasts showed that the molecular families associated with each PARAFAC component are significantly different from one another ($p < 0.0001$).

3.4. Molecular Signature of P1 (Classical Peak A). The 14% of molecular formulas correlated with P1 accounted for 12% of total MS peak intensity (Table 2). P1 formulas were enriched in high MW, high AI_{mod}, low N molecular formulas (Figure 2). Only 9% contained N (Table 2; Figure 1A, and SIS3A), and of all the PARAFAC components, P1 associated formulas were the most enriched in aromatic (27%) and black carbon (17%) compounds, had the highest average MW (536 Da), and the second highest intensity-weighted average MW (397 Da; Table 2). Highly unsaturated compounds accounted for 51% of P1 formulas (Table 2). These formulas likely represented molecules with some terrigenous, aromatic character in these terrestrially dominated river samples (Section 3.2). Thus, together with the aromatic and black carbon moieties, they may contribute directly to the optical properties of P1.

In addition, 58% of all black carbon formulas (65% of summed black carbon peak intensities) and 18% of aromatics (40% of aromatic peak intensities) were associated with P1, indicating that the majority of highly conjugated molecules correlated with this humic-like fluorescence. Black carbon here refers to condensed aromatics formed at high temperature, for instance during forest fires.[40] Once formed, black carbon is ultrabiorefractory, persisting in both soils and the ocean water column for millennia.[41−43] For soils, the main loss term is through dissolution into river waters, where dissolved black carbon constitutes approximately 10% of total DOC.[44−46] In the water column, photodegradation by sunlight is the main identified sink.[23,39] The quantitative significance of black carbon in the soil and riverine carbon cycle, its utility as a tracer of fire-derived organics, and its biostability and photolability, make black carbon an interesting component of the DOM pool to track. Our study shows for the first time that humic-like Peak A may provide an easy-to-measure optical proxy for dissolved black carbon monitoring in natural and impacted waters.

P1 associated molecules spanned the largest extent of van Krevelen space (Figure 1A, SI S3A), MWs (167 to 899 Da), and modified aromaticity index values of any molecular family (Figure 3; Table 2). That such a diversity of molecules track one fluorescent feature demonstrates that FDOM provides a window, not just upon DOM fluorophores, but also a broad family of nonfluorescent molecules that apparently track FDOM in the environment. Molecules within each family may covary with one another and fluorescence across samples due to similarities in their sources and sinks, i.e. they may be biogeochemically related families. However, there may be a more fundamental, chemical reason behind their covariation, particularly in the case of P1.

Early work viewed humic substances as large macromolecules with physically defined MWs sometimes exceeding 1 million Da.[47,48] However, such high MWs are at odds with results from FTICR-MS (MWs <1000 Da; Figure 3)[38] and the apparent macromolecular properties of humics may derive from the aggregation of smaller molecules.[49,50] Coupling liquid chromatography and multidimensional nuclear magnetic resonance (NMR), Simpson et al.[51] postulated that the apparent macromolecular properties observed for humics derive from the aggregation of a mixture of relatively small (< ~ 2000 Da) aliphatics, aromatics, polysaccharides and polypeptides. Therefore, the diverse suite of small molecules tracking P1 may

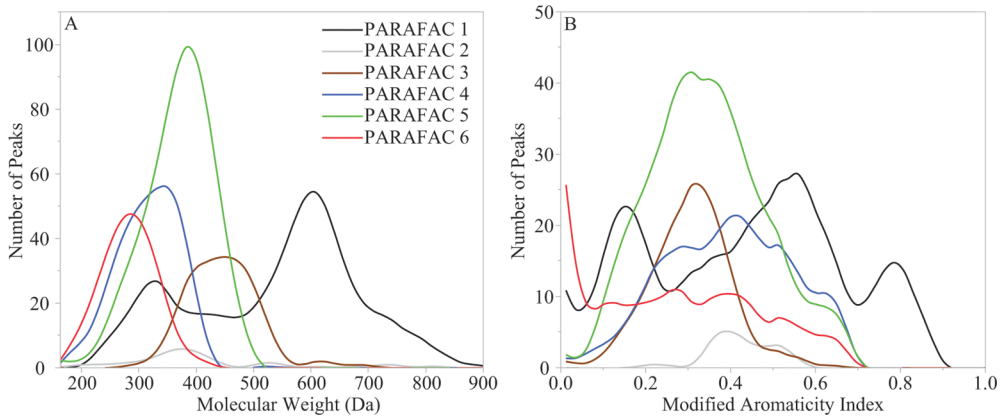

Figure 3. Molecular weight (Panel A) and modified aromaticity index (Panel B) distributions of elemental formulas within each molecular family associated with PARAFAC components 1− 6.

represent the aggregated molecules that en masse have previously been classified as humic substances. The presence of such aggregates could also enhance the dissolution of some of the component compounds, such as black carbon, which might otherwise be expected to have a relatively low solubility.[52] Thus, molecular trends for P1 are consistent with reports that humic Peak A represents an aggregation of highly diverse, relatively high MW (still below 1000 Da), carbon-rich, nitrogen-poor, terrigenous molecules.[9,12,33,51]

3.5. Molecular Signature of P2 (Unknown Humic-Like). Only 1% percent of formulas correlated with P2 (Table 2). A large fraction of P2 formulas were shared with P3 (39%), the latter defined as humic-like Peak C (Table 3). As for humic-like P1 and P3, P2 was enriched in high MW, high aromaticity and low N molecular formulas (Figure 2; Table 2). Of the formulas assigned to P2, none contained N, 2% were black carbon, 21% aromatics, and 59% highly unsaturated (SI Figure S3B; Table 2). In common with P1, P2 formulas covered a large range in MWs and modified aromaticity index values (Figure 3). In contrast to P1, no aliphatic compounds were associated with P2. Based upon its long wavelength shifted fluorescence, high MW, low N content, and high aromatic content, P2 appears indicative of a form of terrigenous humic-like DOM.

3.6. Molecular Signature of P3 (Primary Maximum Classical Peak C). The 5% of formulas that correlated with P3 (Table 2) tended to be high MW, high aromaticity and low N molecular formulas (Figure 2). The average (445 Da) MW of P3 formulas was less than for P1 formulas, but greater than the average across all formulas (Table 2). The intensity-weighted average MW for P3 formulas (424 Da) was the highest among all families (Table 2). Similarly, P3 formulas were depleted in N compared to all formulas, but enriched in N compared to P1 and P2 molecular families (Table 2; Figure 1B, SI S3C). The tighter mass and aromaticity index distribution of P3 molecules (Figure 3), as well as their tight clustering in van Krevelen space (Figure 1B, SI S3C), indicate a more homogeneous mixture of compounds than associated with P1. The area of van Krevelen space occupied by P3 formulas is consistent with lignin-like compounds, the structural biopolymer widely used as a biomarker for vascular land plants.[37] Lignin-derived phenols are highly photolabile,[53] as was P3.[19] Thus, although depleted in aromatic (4%) and black carbon (<1%; Table 2), P3 molecular traits were consistent with a family of predominantly terrigenous molecules of lower conjugation, lower diversity, and higher N than P1 formulas. Such traits suggest a pool of plant-derived organics that have undergone less reworking in soils and natural waters since production, and are less involved in aggregate formation than P1 formulas.

3.7. Molecular Signature of P4 (Between Peak C and M). The 333 (8%) molecular formulas tracking P4 (Table 2) were enriched in high N, lower MW and lower aromaticity molecules (Figure 2). Aromatics accounted for 25%, black carbon 2%, highly unsaturated compounds 67%, and aliphatics 5% of P4 formulas (Table 2), and P4 formulas were enriched in N (78%) compared to all other PARAFAC components (Table 2). P4 formulas had an average MW of 316 Da and an intensity-weighted average MW of 329 Da (Table 2). P4 formulas were tightly grouped in van Krevelen space (SI Figure S3D), and covered a narrow range of MW and aromaticity index values (Figure 3). In the EEM plot (SI Figure S3D), P4 falls near the classically defined terrigenous Peak C, extending toward marine Peak M. The molecular signatures of P4 formulas suggest a pool of N-enriched, low MW DOM, with modest heterogeneity. This description more closely matches that of classically defined Peak M, than Peak C,[12,31,32] suggesting that P4 is more closely related to Peak M, than Peak C. Peak M is most often associated with marine and other waters where autochthonous or microbial DOM is abundant,[10] but P4 determined here, has been shown to increase during photodegradation of boreal DOM.[19]

3.8. Molecular Signature of P5 (Between Peak M and N). The 14% of molecular formulas associated with P5 (Table 2) constituted 28% of mass spectral intensity, indicating a large number of abundant molecules track P5 (Table 2). The 224 formulas shared with P4 equated to 67% of all P4 formulas (333) or 39% of P5 formulas (572; Table 3). As a result, P4 and P5 fall close to one another in the canonical centroid plot, which shows both molecular families to be enriched in N-containing, low aromaticity, low MW formulas (Figure 2). Average (369 Da) and intensity-weighted average (378 Da) MWs of P5 formulas were lower than the overall average (450 Da; 379 Da), but higher than for P4 (316 Da; 329 Da; Table 2). P5 formulas were depleted in aromatics (13%), contained few condensed aromatics (1%), and were enriched in N (69%) compared to all other PARAFAC components bar P4 (Table 2). As for P4, the distributions of P5 formulas with mass and aromatic index (Figure 3), as well as in van Krevelen space (SI Figure S3E), indicate a pool of chemically related molecules. In summary, the P5 molecular family indicates a pool of N-

enriched, low MW DOM. These characteristics fit well with classical descriptions of fluorescent Peaks M and N,[12,31,32] between which P5 sits in the EEM spectrum (SI Figure S3E).

3.9. Molecular Signature of P6 (Peak B and T). Of the 244 P6 formulas (Table 2), 31% contained N. These relatively low N levels were unexpected as P6 corresponded to protein-like fluorescence Peaks B and T, which correlate with concentrations of hydrolyzable amino acids in natural waters.[54] Use of PPL and negative mode ESI may have discriminated against N-rich compounds.[20,38] However, P6 formulas were of lower N-content than the formulas associated with P4 and P5 in this study, and were not enriched in N compared to bulk DOM detectable via PPL extraction and ESI FTICR-MS (Table 2). This was also apparent in the canonical plot, where P6 formulas were of similar N-content, but of lower MW and aromatic content than the bulk DOM (Figure 2). Peaks B and T optical properties may also stem from low MW, N-free aromatic compounds, such as gallinic acid, which has a strong fluorescence signal in the region of Peaks B and T.[34] Further examination revealed that 75% of the 37 (aromatics) aromatics associated with P6 contained N. Thus, although the total population of molecules tracking P6 is N-depleted, the aromatics are N-enriched; suggesting a significant proportion of P6 fluorescence comes from N-containing aromatics.

Although the compounds responsible for P6 fluorescence require further elucidation, the formulas correlated with P6 had a distinct molecular signature. These P6 formulas had the lowest average (244 Da) and intensity-weighted average (279 Da) MWs, and were enriched in aliphatics (27%) (Table 2; Figure 3, SI S3F). Many P6 formulas do not fluoresce (e.g., many were aliphatic). The above molecular characteristics are consistent with a fresh DOM pool, and reports that Peaks B and T represent the most biolabile fraction of FDOM.[19,55,56]

4. IMPLICATIONS FOR INTERPRETATION OF DOM FLUORESCENCE

Almost 40% of the 4109 molecular formulas identified and 60% of FTICR-MS peak intensities were associated with a PARAFAC component, including nonaromatic compounds, indicating that coupled EEM/PARAFAC analyses offer information not just about the fraction of dissolved organic molecules that fluoresce, but about broader families of biogeochemically related molecules that track one another in the environment. Molecular families associated with PARAFAC components were broadly consistent with previous chemical and ecological interpretations of fluorescence features, offering reassurance to environmental scientists using either fluorescence or FTICR-MS to study DOM. Although encouraging for those using fluorescence to track the bulk pool of DOM, this also highlights the complexity of the molecular underpinnings of fluorescence signatures, and suggests caution should be applied in the interpretation of DOM optical signatures, particularly when moving between systems (e.g., river/glacier/ocean).

Presumably there is a core group of aromatic fluorophores that give rise to the fluorescent properties of DOM. Defining these fluorophores is important to develop a mechanistic understanding of DOM optical properties and the caveats involved in utilizing fluorophores to define the unseen molecules with which they covary. Isolating and characterizing the elemental, structural and optical properties of each dissolved organic molecule present in a natural water sample is a major, perhaps impossible task. Even with such information, a complete, reductionist understanding of DOM optical properties may remain beyond reach as each fluorescent molecule's optical properties are also altered by the environmental matrix in which they are dissolved—not least the other organics present.[57] This is apparent when considering that the molecules giving rise to classical humic Peak A, may not represent a large macromolecule (>thousands of Da) with diverse functional moieties, but an aggregation of loosely associated small (∼<2000 Da) molecules, perhaps held in association with cations such as iron.[51] Thus, some of the fluorescent properties of DOM should be considered an emergent property of the milieu of fluorophoric and non-fluorophoric, organic and inorganic compounds, dissolved in natural waters.

Other processes may also cause covariation between fluorescent and nonfluorescent molecules. Covariation may be related to a common origin and cotransport of molecular families from land to the aquatic environment. It is possible that covariation reflects not only this passive cotransport, but also a common cycling. For example, humic-like and protein-like FDOM components are both consumed and produced by microbes and abiotic photochemistry in laboratory incubations.[19,58] Consequently, the net change of these components is a function of both intrinsic DOM properties, such as origin and lability, and the factors that influence microbial metabolism (e.g., nutrients)[58] and photochemistry (e.g., light field).[17] Fluorescent components vary greatly with respect to their photoreactivity: components such as Peak A and C (here the equivalent of P1 and P3) are quickly removed by light; while others, such as P4, may be produced.[19] It is more difficult to conceptualize the covariation in this scenario, because non-colored molecules are intrinsically less reactive to light. That said, FTICR-MS data for photoirradiated Congo River water revealed that a broad suite of dissolved organics, including noncolored aliphatics, were photolabile,[23] possibly due to secondary photoreactions. It is further possible, that some of the covarying molecular families may be bio- or photo-degradation products of the actual fluorophores. These different processes probably coexist. Understanding the mechanistic basis of the molecular correlates of PARAFAC components will help understand and more effectively predict the links that have been observed between the optical properties of DOM and its biological and photochemical reactivity, a key element in our understanding of aquatic ecosystem function, including CO_2 dynamics and emissions.[27]

As with any empirical correlation, the molecular families described should not be regarded as universally associating with each PARAFAC component. In different systems, where the dissolved organic milieu is the result of different sources and processes, the molecular family tracking a fluorescence component may differ from those detailed here. Thus, further work is required to determine variability in the chemistry and ecological functions of the larger suite of dissolved organic molecules that track specific fluorescence features in a variety of natural waters.

The optical and molecular signatures of the 22 DOM samples studied were broadly representative of DOM in other freshwater samples, including the 1349 samples in the PARAFAC analysis that yielded the six fluorescence components to which molecular families were ascribed. Consequently, the trends presented here provide a guide as to the qualities of seen and unseen molecules that track the commonly identified DOM fluorescence features in natural waters.

■ ASSOCIATED CONTENT

Supporting Information

The Supporting Information contains extended methods (Section S1a-c), three figures (Figure S1, S2 and S3), and two tables (Table S1 and S2). This material is available free of charge via the Internet at http://pubs.acs.org/.

■ AUTHOR INFORMATION

Corresponding Author

*Phone: +1(912)598-2320; fax: +1(912)598-2310; e-mail: aron.stubbins@skio.uga.edu.

Notes

The authors declare no competing financial interest.

■ ACKNOWLEDGMENTS

We thank Annick St-Pierre, Alice Parkes and the CarBBAS team for sampling assistance, and Katrin Klaproth for technical support. Support provided by the Natural Sciences and Engineering Research Council of Canada and Hydro-Québec through the Industrial Research Chair on Carbon Biogeochemistry in Boreal Aquatic Systems (CarBBAS) to del Giorgio, the National Science Foundation (OCE-1234704; DEB-1146161), and a Fellowship from the Hanse Institute for Advanced Studies (HWK, Delmenhorst, Germany) granted to Stubbins.

■ REFERENCES

(1) Prairie, Y. T. Carbocentric limnology: Looking back, looking forward. *Can. J. Fish. Aquat. Sci.* **2008**, *65* (3), 543−548.

(2) Morris, D. P.; Zagarese, H.; Williamson, C. E.; Balseiro, E. G.; Hargreaves, B. R.; Modenutti, B.; Moeller, R.; Queimalinos, C. The attentuation of solar UV radiation in lakes and the role of dissolved organic carbon. *Limnol. Oceanogr.* **1995**, *40* (8), 1381−1391.

(3) Mopper, K.; Kieber, D. J.; Stubbins, A., Marine photochemistry: Processes and impacts. In *Biogeochemistry of Marine Dissolved Organic Matter*, 2nd ed.; Hansell, D. A., Carlson, C. A., Ed.; Elsevier, 2014; DOI: 10.1016/B978-0-12-405940-5.00008-X.

(4) Ravichandran, M. Interactions between mercury and dissolved organic matter - a review. *Chemosphere* **2004**, *55* (3), 319−331.

(5) Haitzer, M.; Hoss, S.; Traunspurger, W.; Steinberg, C. Effects of dissolved organic matter (DOM) on the bioconcentration of organic chemicals in aquatic organisms - A review. *Chemosphere* **1998**, *37* (7), 1335−1362.

(6) Dittmar, T.; Stubbins, A. *Dissolved Organic Matter in Aquatic Systems in Treatise of Geochemistry*; Birrer, B., Falkowski, P., Freeman, K., Ed.; Elsevier, 2014; pp 125−156.

(7) Weishaar, J. L.; Aiken, G. R.; Bergamaschi, B. A.; Fram, M. S.; Fujii, R.; Mopper, K. Evaluation of specific ultraviolet absorbance as an indicator of the chemical composition and reactivity of dissolved organic carbon. *Environ. Sci. Technol.* **2003**, *37* (20), 4702−4708.

(8) Stubbins, A.; Hubbard, V.; Uher, G.; Law, C. S.; Upstill-Goddard, R. C.; Aiken, G. R.; Mopper, K. Relating carbon monoxide photoproduction to dissolved organic matter functionality. *Environ. Sci. Technol.* **2008**, *42* (9), 3271−3276.

(9) Coble, P. G.; Green, S. A.; Blough, N. V.; Gagosian, R. B. Characterization of dissolved organic-matter in the black-sea by fluorescence spectroscopy. *Nature* **1990**, *348* (6300), 432−435.

(10) Coble, P. G. Characterization of marine and terrestrial DOM in seawater using excitation emission matrix spectroscopy. *Mar. Chem.* **1996**, *51* (4), 325−346.

(11) Cory, R. M.; McKnight, D. M. Fluorescence spectroscopy reveals ubiquitous presence of oxidized and reduced quinones in dissolved organic matter. *Environ. Sci. Technol.* **2005**, *39* (21), 8142−8149.

(12) Fellman, J. B.; Hood, E.; Spencer, R. G. M. Fluorescence spectroscopy opens new windows into dissolved organic matter dynamics in freshwater ecosystems: A review. *Limnol. Oceanogr.* **2010**, *55* (6), 2452−2462.

(13) Ishii, S. K. L.; Boyer, T. H. Behavior of reoccurring PARAFAC components in fluorescent dissolved organic matter in natural and engineered systems: A critical review. *Environ. Sci. Technol.* **2012**, *46* (4), 2006−2017.

(14) Stedmon, C. A.; Bro, R. Characterizing dissolved organic matter fluorescence with parallel factor analysis: A tutorial. *Limnol. Oceanogr.: Methods* **2008**, *6*, 572−579.

(15) Kujawinski, E. B.; Del Vecchio, R.; Blough, N. V.; Klein, G. C.; Marshall, A. G. Probing molecular-level transformations of dissolved organic matter: Insights on photochemical degradation and protozoan modification of DOM from electrospray ionization Fourier transform ion cyclotron resonance mass spectrometry. *Mar. Chem.* **2004**, *92* (1−4), 23−37.

(16) Hertkorn, N.; Benner, R.; Frommberger, M.; Schmitt-Kopplin, P.; Witt, M.; Kaiser, K.; Kettrup, A.; Hedges, J. I. Characterization of a major refractory component of marine dissolved organic matter. *Geochim. Cosmochim. Acta* **2006**, *70* (12), 2990−3010.

(17) Stubbins, A.; Law, C. S.; Uher, G.; Upstill-Goddard, R. C. Carbon monoxide apparent quantum yields and photoproduction in the Tyne estuary. *Biogeosciences* **2011**, *8* (3), 703−713.

(18) Hu, C. M.; Muller-Karger, F. E.; Zepp, R. G. Absorbance, absorption coefficient, and apparent quantum yield: A comment on common ambiguity in the use of these optical concepts. *Limnol. Oceanogr.* **2002**, *47* (4), 1261−1267.

(19) Lapierre, J.-F.; del Giorgio, P. A. Partial coupling and differential regulation of biologically and photo-chemically labile dissolved organic carbon across boreal aquatic networks. *Biogeosciences Discuss.* **2014**, DOI: 10.5194/bgd-11-6673-2014.

(20) Dittmar, T.; Koch, B.; Hertkorn, N.; Kattner, G. A simple and efficient method for the solid-phase extraction of dissolved organic matter (SPE-DOM) from seawater. *Limnol. Oceanogr.: Methods* **2008**, *6*, 230−235.

(21) Singer, G. A.; Fasching, C.; Wilhelm, L.; Niggemann, J.; Steier, P.; Dittmar, T.; Battin, T. J. Biogeochemically diverse organic matter in Alpine glaciers and its downstream fate. *Nat. Geosci.* **2012**, *5* (10), 710−714.

(22) Koch, B. P.; Dittmar, T.; Witt, M.; Kattner, G. Fundamentals of molecular formula assignment to ultrahigh resolution mass data of natural organic matter. *Anal. Chem.* **2007**, *79* (4), 1758−1763.

(23) Stubbins, A.; Spencer, R. G. M.; Chen, H. M.; Hatcher, P. G.; Mopper, K.; Hernes, P. J.; Mwamba, V. L.; Mangangu, A. M.; Wabakanghanzi, J. N.; Six, J. Illuminated darkness: Molecular signatures of Congo River dissolved organic matter and its photochemical alteration as revealed by ultrahigh precision mass spectrometry. *Limnol. Oceanogr.* **2010**, *55* (4), 1467−1477.

(24) Santl-Temkiv, T.; Finster, K.; Dittmar, T.; Hansen, B. M.; Thyrhaug, R.; Nielsen, N. W.; Karlson, U. G., Hailstones: A window into the microbial and chemical inventory of a storm cloud. *PLoS One* **2013**, *8*, (1).

(25) Koch, B. P.; Dittmar, T. From mass to structure: An aromaticity index for high-resolution mass data of natural organic matter. *Rapid Commun. Mass Spectrom.* **2006**, *20* (5), 926−932.

(26) Lapierre, J. F.; del Giorgio, P. A., Geographical and environmental drivers of regional differences in the lake pCO_2 versus DOC relationship across northern landscapes. *J. Geophys. Res.: Biogeosci.* **2012**, *117*, DOI: 10.1029/2012JG001945.

(27) Lapierre, J. F.; Guillemette, F.; Berggren, M.; del Giorgio, P. A., Increases in terrestrially derived carbon stimulate organic carbon processing and CO2 emissions in boreal aquatic ecosystems. *Nat. Commun.* **2013**, *4*.

(28) Spencer, R. G. M.; Butler, K. D.; Aiken, G. R., Dissolved organic carbon and chromophoric dissolved organic matter properties of rivers in the USA. *J. Geophys. Res.: Biogeosci.* **2012**, *117*.

(29) Mulholland, P. J., Large scale patterns in DOC concentration, flux, and sources. In *Aquatic Ecosystems: Interactivity of Dissolved Organic Matter*; Findlay, S., Sinsabaugh, R., Ed. ; Elsevier, 2003; pp 139−159.

(30) Stubbins, A.; Uher, G.; Law, C. S.; Mopper, K.; Robinson, C.; Upstill-Goddard, R. C. Open-ocean carbon monoxide photoproduction. *Deep Sea Res., Part II* **2006**, *53* (14−16), 1695−1705.
(31) Romera-Castillo, C.; Nieto-Cid, M.; Castro, C. G.; Marrase, C.; Largier, J.; Barton, E. D.; Alvarez-Salgado, X. A. Fluorescence: Absorption coefficient ratio - Tracing photochemical and microbial degradation processes affecting coloured dissolved organic matter in a coastal system. *Mar. Chem.* **2011**, *125* (1−4), 26−38.
(32) Romera-Castillo, C.; Sarmento, H.; Alvarez-Salgado, X. A.; Gasol, J. M.; Marrase, C. Net production and consumption of fluorescent colored dissolved organic matter by natural bacterial assemblages growing on marine phytoplankton exudates. *Appl. Environ. Microbiol.* **2011**, *77* (21), 7490−7498.
(33) Coble, P. G.; Del Castillo, C. E.; Avril, B. Distribution and optical properties of CDOM in the Arabian Sea during the 1995 Southwest Monsoon. *Deep Sea Res., Part II* **1998**, *45* (10−11), 2195−2223.
(34) Maie, N.; Scully, N. M.; Pisani, O.; Jaffé, R. Composition of a protein-like fluorophore of dissolved organic matter in coastal wetland and estuarine ecosystems. *Water Res.* **2007**, *41* (3), 563−570.
(35) Ward, N. D.; Keil, R. G.; Medeiros, P. M.; Brito, D. C.; Cunha, A. C.; Dittmar, T.; Yager, P. L.; Krusche, A. V.; Richey, J. E. Degradation of terrestrially derived macromolecules in the Amazon River. *Nat. Geosci.* **2013**, *6* (7), 530−533.
(36) Ertel, J. R.; Hedges, J. I.; Perdue, E. M. Lignin signature of aquatic humic substances. *Science* **1984**, *223* (4635), 485−487.
(37) Liu, Z. F.; Sleighter, R. L.; Zhong, J. Y.; Hatcher, P. G. The chemical changes of DOM from black waters to coastal marine waters by HPLC combined with ultrahigh resolution mass spectrometry. *Estuarine, Coastal Shelf Sci.* **2011**, *92* (2), 205−216.
(38) Mopper, K.; Stubbins, A.; Ritchie, J. D.; Bialk, H. M.; Hatcher, P. G. Advanced instrumental approaches for characterization of marine dissolved organic matter: Extraction techniques, mass spectrometry, and nuclear magnetic resonance spectroscopy. *Chem. Rev.* **2007**, *107* (2), 419−442.
(39) Stubbins, A.; Niggemann, J.; Dittmar, T. Photo-lability of deep ocean dissolved black carbon. *Biogeosciences* **2012**, *9* (5), 1661−1670.
(40) Forbes, M. S.; Raison, R. J.; Skjemstad, J. O. Formation, transformation and transport of black carbon (charcoal) in terrestrial and aquatic ecosystems. *Sci. Total Environ.* **2006**, *370* (1), 190−206.
(41) Dittmar, T.; Paeng, J. A heat-induced molecular signature in marine dissolved organic matter. *Nat. Geosci.* **2009**, *2* (3), 175−179.
(42) Ziolkowski, L. A.; Druffel, E. R. M., Aged black carbon identified in marine dissolved organic carbon. *Geophys. Res. Lett.* **2010**, *37*.
(43) Schmidt, M. W. I.; Torn, M. S.; Abiven, S.; Dittmar, T.; Guggenberger, G.; Janssens, I. A.; Kleber, M.; Kogel-Knabner, I.; Lehmann, J.; Manning, D. A. C.; Nannipieri, P.; Rasse, D. P.; Weiner, S.; Trumbore, S. E. Persistence of soil organic matter as an ecosystem property. *Nature* **2011**, *478* (7367), 49−56.
(44) Dittmar, T.; de Rezende, C. E.; Manecki, M.; Niggemann, J.; Ovalle, A. R. C.; Stubbins, A.; Bernardes, M. C. Continuous flux of dissolved black carbon from a vanished tropical forest biome. *Nat. Geosci.* **2012**, *5* (9), 618−622.
(45) Jaffe, R.; Ding, Y.; Niggemann, J.; Vahatalo, A. V.; Stubbins, A.; Spencer, R. G. M.; Campbell, J.; Dittmar, T. Global charcoal mobilization from soils via dissolution and riverine transport to the oceans. *Science* **2013**, *340* (6130), 345−347.
(46) Guggenberger, G.; Rodionov, A.; Shibistova, O.; Grabe, M.; Kasansky, O. A.; Fuchs, H.; Mikheyeva, N.; Zrazhevskaya, G.; Flessa, H. Storage and mobility of black carbon in permafrost soils of the forest tundra ecotone in Northern Siberia. *Global Change Biol.* **2008**, *14* (6), 1367−1381.
(47) Schulten, H. R.; Schnitzer, M. A State-of-the-Art Structural Concept for Humic Substances. *Naturwissenschaften* **1993**, *80* (1), 29−30.
(48) Swift, R. S., Molecular weight, size, shape, and charge characteristics of humic substances: Some basic considerations. In *Humic substances. II. In Search of Structure*; Hayes, M. H. B., MacCarthy, P., Malcolm, R. L., Swift, R. S., Ed.; Wiley: Chichester, 1989; pp 449−466.
(49) Piccolo, A.; Nardi, S.; Concheri, G. Micelle-like conformation of humic substances as revealed by size exclusion chromatography. *Chemosphere* **1996**, *33* (4), 595−602.
(50) Wershaw, R. L. Molecular aggregation of humic substances. *Soil Sci.* **1999**, *164* (11), 803−813.
(51) Simpson, A. J.; Kingery, W. L.; Hayes, M. H. B.; Spraul, M.; Humpfer, E.; Dvortsak, P.; Kerssebaum, R.; Godejohann, M.; Hofmann, M. Molecular structures and associations of humic substances in the terrestrial environment. *Naturwissenschaften* **2002**, *89* (2), 84−88.
(52) Perminova, I. V.; Grechishcheva, N. Y.; Petrosyan, V. S. Relationships between structure and binding affinity of humic substances for polycyclic aromatic hydrocarbons: Relevance of molecular descriptors. *Environ. Sci. Technol.* **1999**, *33* (21), 3781−3787.
(53) Spencer, R. G. M.; Stubbins, A.; Hernes, P. J.; Baker, A.; Mopper, K.; Aufdenkampe, A. K.; Dyda, R. Y.; Mwamba, V. L.; Mangangu, A. M.; Wabakanghanzi, J. N.; Six, J., Photochemical degradation of dissolved organic matter and dissolved lignin phenols from the Congo River. *J. Geophys. Res.: Biogeosci.* **2009**, *114*.
(54) Yamashita, Y.; Tanoue, E. Chemical characterization of protein-like fluorophores in DOM in relation to aromatic amino acids. *Mar. Chem.* **2003**, *82* (3−4), 255−271.
(55) Stedmon, C. A.; Markager, S. Tracing the production and degradation of autochthonous fractions of dissolved organic matter by fluorescence analysis. *Limnol. Oceanogr.* **2005**, *50* (5), 1415−1426.
(56) Jorgensen, L.; Stedmon, C. A.; Kragh, T.; Markager, S.; Middelboe, M.; Sondergaard, M. Global trends in the fluorescence characteristics and distribution of marine dissolved organic matter. *Mar. Chem.* **2011**, *126* (1−4), 139−148.
(57) Pace, M. L.; Reche, I.; Cole, J. J.; Fernandez-Barbero, A.; Mazuecos, I. P.; Prairie, Y. T. pH change induces shifts in the size and light absorption of dissolved organic matter. *Biogeochemistry* **2012**, *108* (1−3), 109−118.
(58) Guillemette, F.; del Giorgio, P. A. Simultaneous consumption and production of fluorescent dissolved organic matter by lake bacterioplankton. *Environ. Microbiol.* **2012**, *14* (6), 1432−1443.